Food Microbiology 113 (2023) 104252

Contents lists available at ScienceDirect

Food Microbiology

journal homepage: www.elsevier.com/locate/fm

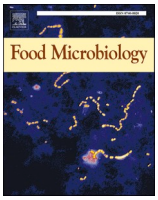

Susceptibility and transcriptomic response to plasma-activated water of *Listeria monocytogenes* planktonic and sessile cells

Paula Fernández-Gómez [a,*], José F. Cobo-Díaz [a], Marcia Oliveira [a], Montserrat González-Raurich [a], Avelino Alvarez-Ordóñez [a], Miguel Prieto [a], James L. Walsh [b], Morten Sivertsvik [c], Estefanía Noriega-Fernández [c,d,1], Mercedes López [a,1]

[a] Department of Food Hygiene and Technology, Universidad de León, León, Spain
[b] Centre for Plasma Microbiology, University of Liverpool, UK
[c] Department of Processing Technology, Nofima AS, Stavanger, Norway
[d] European Food Safety Authority (EFSA), Parma, Italy

ARTICLE INFO

Keywords:
Plasma-activated water
Antimicrobial activity
Listeria monocytogenes
Transcriptomics
Anti-Biofilm

ABSTRACT

Plasma-Activated Water (PAW) was generated from tap water using a surface dielectric barrier discharge at different discharge power (26 and 36 W) and activation time (5 and 30 min). The inactivation of a three-strain *Listeria monocytogenes* cocktail in planktonic and biofilm state was evaluated. PAW generated at 36 W-30 min showed the lowest pH and the highest hydrogen peroxide, nitrates, nitrites contents and effectiveness against cells on planktonic state, resulting in 4.6 log reductions after a 15-min treatment. Although the antimicrobial activity in biofilms formed on stainless steel and on polystyrene was lower, increasing the exposure time to 30 min allowed an inactivation >4.5 log cycles. The mechanisms of action of PAW were investigated using chemical solutions that mimic its physico-chemical characteristics and also RNA-seq analysis. The main transcriptomic changes affected carbon metabolism, virulence and general stress response genes, with several overexpressed genes belonging to the cobalamin-dependent gene cluster.

1. Introduction

Microbial ability to adhere to surfaces and form biofilms, i.e. structured communities that grow surrounded by a self-produced matrix of extracellular polymeric substances (EPS), greatly contributes to their persistence in food processing environments. Biofilms are a potential source of cross-contamination with both spoilage and pathogenic microorganisms (Alvarez-Ordóñez et al., 2019; Bridier et al., 2015), such as *Listeria monocytogenes*, a foodborne opportunistic pathogen causing listeriosis, one of the most serious foodborne diseases under EU surveillance (EFSA and ECDC, 2021).

An efficient sanitization program in the food industry is essential to avoid food contamination and ensure the microbial safety and quality of the final product. However, bacteria within biofilms show an enhanced tolerance to different types of stress conditions, including increased resistance to commonly used disinfectants, which reduces the efficacy of cleaning and disinfection processes and challenges the inactivation of target microorganisms and, eventually, the complete removal of biofilms (Li et al., 2021; Sanchez-Vizuete et al., 2015; Günther et al., 2016).

In the last decade, intense research efforts have focused on the development of more environmentally friendly sanitation and biofilm control strategies with enhanced effectiveness in biofilm removal while not promoting the development of bacterial resistance (Hua et al., 2019; Mazaheri et al., 2021). Plasma activated water (PAW), generated through the exposure of water to non-thermal atmospheric plasma, has emerged as a promising alternative to traditional sanitisers in the food industry (López et al., 2019; Oliveira et al., 2022), given its potential for sustainable production, offsite generation and storability (Herianto et al., 2021; Zhao et al., 2020a).

PAW has shown a great potential for decontamination of food

* Corresponding author.
E-mail addresses: pafeg@unileon.es (P. Fernández-Gómez), jcobd@unileon.es (J.F. Cobo-Díaz), msouo@unileon.es (M. Oliveira), mmgonr@unileon.es (M. González-Raurich), aalvo@unileon.es (A. Alvarez-Ordóñez), miguel.prieto@unileon.es (M. Prieto), jlwalsh@liverpool.ac.uk (J.L. Walsh), morten.sivertsvik@nofima.no (M. Sivertsvik), Estefania.NORIEGAFERNANDEZ@efsa.europa.eu (E. Noriega-Fernández), mmlopf@unileon.es (M. López).
[1] These authors equally contributed to the work.

https://doi.org/10.1016/j.fm.2023.104252
Received 29 September 2022; Received in revised form 5 March 2023; Accepted 6 March 2023
Available online 7 March 2023

products and food processing environments and a wide spectrum of antimicrobial activity, which has been attributed to a synergistic action of its often low pH and the reactive oxygen and nitrogen species (RONS) that result from the interaction of plasma-generated active particles, e.g. ions or free radicals, with water molecules (Naítali et al., 2010; Zhou et al., 2018). PAW composition and inactivation efficacy have been related to multiple parameters such as water source, plasma system (e.g. atmospheric pressure plasma jet, dielectric barrier discharge), electrode configuration, precursor gas and activation conditions (e.g. voltage, frequency, flow rate, plasma power, activation time) (Mai-Prochnow et al., 2021).

Several studies have demonstrated the efficacy of PAW for the inactivation of planktonic cells, but there is less information available on its effectiveness against sessile cells in biofilms that often show higher resistance towards treatment (Hozák et al., 2018; Zhao et al., 2020a). The reason of this protective effect has been frequently attributed to the physical structure of the biofilm, with a high cell density and the presence of the EPS matrix, but it can also be related to the physiological state of the cells, since biofilms contain heterogenic subpopulations regarding gene expression and metabolic activities. PAW might also interfere with quorum sensing bacterial communication systems and damage the EPS matrix leading to a physical release of cells, but the precise mode of action is still unclear (Mai-Prochnow et al., 2021). Likewise, more detailed studies regarding PAW chemistry, stability, inactivation mechanisms and influence of generation conditions are still required towards technology upscaling and industrial uptake. There is also scarcity of studies regarding the effect of PAW treatments on bacterial gene expression, and the few ones available have been performed through real time polymerase chain reaction (RT-PCR), focusing exclusively on certain genes of interest (Ercan et al., 2018; Li et al., 2019; Yost and Joshi, 2015). High-throughput transcriptomic tools such as RNA-sequencing (RNA-seq), which are still relatively novel in the food microbiology field, can provide further insight regarding PAW mechanisms of action and possible impacts, in terms of expression of bacterial resistance and virulence phenotypes (Casey et al., 2014; Lamas et al., 2019; Smet et al., 2019). In the particular case of *L. monocytogenes*, the antimicrobial activity of PAW has been previously reported on planktonic cells (Baek et al., 2019), inoculated food products (Machado-Moreira et al., 2021) and biofilms (Handorf et al., 2021; Smet et al., 2019), while the effects on gene expression have been only assessed by RT-PCR for cold plasma treatments (Cui et al., 2021; Patange et al., 2019), and, to our knowledge, not yet for PAW.

In this study, the influence of some PAW generation conditions (plasma power and activation time) on its physico-chemical composition (pH and concentration of hydrogen peroxide, nitrates and nitrites) and efficacy against *L. monocytogenes* planktonic cells was initially evaluated. Then, the most effective PAW was selected to study its capacity to eliminate *L. monocytogenes* biofilms on stainless steel and polystyrene. PAW inactivation mechanisms were explored on *L. monocytogenes* planktonic cells by applying different chemical solutions that partially mimic the concentration of PAW reactive species and/or its pH. Moreover, the transcriptomic response to PAW of planktonic and sessile cells of a *L. monocytogenes* strain was studied through RNA-seq based gene expression analysis.

2. Materials and methods

2.1. Bacterial strains, media and culture conditions

L. monocytogenes strains used in this study were two strains isolated from a meat industry (ULE1264, serotype 1/2a, and ULE1265, serotype 1/2c NCBI GenBank JALDPS000000000) and a reference strain from the Spanish Type Culture Collection (CECT 911, serotype 1/2c). The master stocks of all strains were maintained at −20 °C in cryovials with 40% v/v of glycerol as cryoprotectant. The strains were recovered by streaking them on Brain Heart Infusion (BHI, Merck, USA) agar plates for a culture purity visual check. After incubation at 37 °C for 24 h, the plates were stored at 4 °C until further use. Then, a single colony was transferred from the plates into 10 mL of fresh BHI broth, followed by incubation at 37 °C for 24 h to obtain stationary phase pre-cultures with a cell density of approximately 10^9 CFU/mL. The individual pre-cultures of the three *L. monocytogenes* strains were mixed in equal volumes in order to obtain a cocktail used for direct exposure to PAW/chemical solutions or to grow biofilms on polystyrene or stainless-steel plates, as described in the next sections.

2.2. PAW generating system and operating conditions

PAW was produced with a cold plasma reactor set to generate a surface dielectric barrier discharge (SDBD) as previously described by Vaka et al. (2019) and Sharmin et al. (2021a,b),b). The system consisted of a powered and a ground electrode separated by a 1 mm-thick quartz disc and coupled to the lid of a treatment chamber with dimensions 176 × 174 × 48 mm (total discharge area of 306.2 cm^2). PAW was generated through the activation of 100 mL of tap water (3.2 mm water column) per run at an initial temperature of 9–11 °C, keeping a gap distance between the liquid surface and the electrode of 44.8 mm. More information regarding the origin and composition of the tap water used to generate PAW can be found in Table S1. During the activation, the system was completely sealed and the water was stirred using evenly distributed magnetic bars. The cold plasma generating source produced a sinusoidal signal at a frequency of 18 kHz and the system operated at atmospheric pressure with ambient air as precursor gas, modifying the power dissipated by the plasma (plasma power). A plasma power of either 26 W (low mode, LM) or 36 W (high mode, HM), and an activation time of 5 or 30 min, were used in the following combinations: low mode discharge power and 5 min of activation (PAW LM5), low mode discharge power and 30 min of activation (PAW LM30) and high mode discharge power and 30 min of activation (PAW HM30).

The generated PAW was stored at 4 °C in sterile flasks until its application on the inactivation assays, which took place 24 h later. This storage conditions have been previously reported to maintain unaffected the pH, nitrates and nitrites levels of this PAW for up to two weeks (Vaka et al., 2019).

2.3. Determination of PAW physico-chemical properties

The pH of PAW and tap water was measured with a FiveGo pH meter (Mettler Toledo, USA). Nitrate and nitrite concentrations were determined with standard spectrophotometric methods using a Shimadzu UVmini-1240-UV-VIS spectrophotometer (Shimadzu, Tokyo, Japan). Nitrate levels were determined with the Spectroquant® test kit for Nitrates #109713 (Merck) at a wavelength of 548 nm. Nitrite levels were measured following the Griess method (Griess, 1879) at a wavelength of 340 nm. Hydrogen peroxide concentrations were determined using the ferric-xylenol orange assay as modified by Gay and Gebicki (2000), with spectrophotometric determination at a wavelength of 560 nm. For the quantification of reactive species, calibration curves for nitrates (0.5–100.0 mg/L), nitrites (0.01–3.00 mg/L) and hydrogen peroxide (25–250 μM), with distilled water as blank, were used. For all determinations, PAW samples were tempered at 15–20 °C, appropriate dilutions were prepared with distilled water and measurements were performed in triplicate.

2.4. Evaluation of PAW inactivation efficacy on L. monocytogenes planktonic cells

For the screening of the antimicrobial activity of PAW on planktonic cells, 0.1 mL of the stationary-phase *L. monocytogenes* cocktail was added to 10 mL of the different PAWs or tap water. Exposure times of 5, 15, 30 and 60 min were tested in duplicate. The treatments were stopped by centrifuging at 8000×*g* for 5 min at 4 °C and resuspending the pellets in

10 mL of a neutralizing solution (Tween 80 (Scharlau, Spain) 10 g/L, L-histidine (Sigma-Aldrich, USA) 0.5 g/L, lecithin (VWR, USA) 1 g/L, $Na_2S_2O_3$ (Panreac, Spain) 2.5 g/L in PBS (Biosciences, USA), pH 7.0). *L. monocytogenes* cells were enumerated by spread-plating 0.1 mL of the appropriately diluted suspensions in Ringer solution (Merck) on BHI agar plates, which were incubated at 37 °C for 24 h.

2.5. Assessment of PAW's mode of antimicrobial action with chemical cocktails

The contribution of NO_2^-, NO_3^-, H_2O_2 and acidic pH to the antimicrobial activity of PAW was investigated using chemical solutions partially mimicking the concentration of reactive species and/or pH in PAW HM30 as follows: "pH 2.3", "NO_2^- + NO_3^-", "H_2O_2" and "NO_2^- + NO_3^- + H_2O_2 + pH 2.3". These solutions were prepared from 10X stocks of $NaNO_2$ (VWR) and $NaNO_3$ (VWR), and a 100X stock of H_2O_2 (from a 30% w/w hydrogen peroxide solution, Sigma-Aldrich). When necessary, the pH was adjusted to 2.3 (pH of PAW HM30) with HCl 0.05 N. The final solutions were sterilized by filtration with a pore size of 0.2 μL. The antimicrobial assays were performed on planktonic cells by adding 0.1 mL of the stationary-phase *L. monocytogenes* cocktail to 10 mL of the different chemical solutions in duplicate, followed by a 30 min exposure. As previously described, the treatments were stopped by centrifugation followed by resuspension of the pellets in the neutralizing solution, and survivors were enumerated by viable plate counting on BHI agar plates.

2.6. Evaluation of PAW inactivation efficacy on L. monocytogenes biofilms formed on stainless steel (SS) and polystyrene

The inactivation efficacy of PAW HM30 was evaluated against *L. monocytogenes* biofilms formed on 35 mm diameter stainless steel and polystyrene plates. For biofilm formation, the stationary-phase *L.monocytogenes* cocktail was 100-fold diluted in fresh BHI broth and 4 mL of the obtained bacterial suspension (~10^7 CFU/mL) were inoculated in each plate. After 6 days at 12 °C, the plates were washed three times with 5 mL Ringer solution and allowed to dry for approximately 20 min and then, 5 mL of PAW were applied per plate. Exposure times of 15, 30 and 60 min, with four independent replicates per time, were tested. Afterwards, PAW was poured off and the plates were inoculated with 5 mL of the neutralization solution and incubated for 2 min at room temperature. Biofilm cells were recovered by rubbing the plate surface with sterile cotton tipped wooden swabs, which were resuspended in 10 mL of Ringer solution and vortexed for 60 s. *L. monocytogenes* cells were enumerated by spread-plating 0.1 mL of the appropriately diluted suspensions in Ringer solution on BHI agar plates, which were incubated at 37 °C for 24 h.

The *D*-value, defined as the time required to obtain an inactivation of 90% of the bacterial population, was calculated for the different assayed conditions as the negative reciprocal of the slope of the fitted line on the plot of $\log_{10}$ CFU/cm^2 against the exposition time in minutes.

2.7. PAW treatment for RNA-seq analysis on planktonic cells and biofilms

For the RNA-seq assay on planktonic cells, 1 mL of the stationary-phase pre-culture of *L. monocytogenes* ULE1265 was inoculated in 100 mL of BHI broth and incubated for 6 days at 12 °C and 100 rpm. Afterwards, 10 mL of a 1:10 dilution of the previous culture in Ringer solution was harvested by centrifugation at 5000×*g* for 5 min and the pellet resuspended in 10 mL of PAW HM30 or Ringer solution for 5 min at room temperature. Immediately after the treatment, the samples were centrifuged at 5000×*g* for 5 min at 4 °C and the pellets were resuspended in 2 mL of RNAprotect (Qiagen, Germany).

For the treatment on biofilms, the stationary-phase pre-culture of *L. monocytogenes* ULE1265 was 100-fold diluted in fresh BHI broth and 4 mL of the bacterial suspension (~10^7 CFU/mL) was distributed on a 35 mm diameter stainless steel plate. After 6 days at 12 °C, the plates were washed three times with 5 mL Ringer solution, allowed to dry for approximately 20 min, and then 5 mL of PAW or Ringer solution were applied to the biofilms for 15 min. After the treatment, the PAW or Ringer solution were discarded, 2 mL of RNAprotect was added to each plate and the biofilm cells were recovered by surface rubbing. Recovered cells from the four replicates were pooled together.

Three independent replicates, from different pre-cultures, were performed for each experimental condition, resulting in three independent RNA extractions per condition.

2.8. RNA extraction and sequencing

RNA was extracted with the RNeasy® Mini Kit (Qiagen) including a previous physical lysis step. First, the RNAprotect was removed by centrifugation at 5000×*g* for 5 min, the cell pellets were resuspended in 600 μL of RLT buffer (from the RNeasy kit) and transferred to Pathogen Lysis Tubes S (Qiagen). After 20 min vortexing, 400 μL of the lysate was mixed with 400 μL of 70% v/v ethanol to continue with the RNA extraction following the manufacturer's instructions. RNA concentration in the final preparation was measured with a Qubit 3.0 fluorometer (Invitrogen, USA) using the fluorometric assay Qubit™ RNA Extended Range (XR) Assay Kit (Invitrogen). RNA samples were kept at −80 °C until further use for sequencing. Libraries for sequencing were prepared using Illumina Stranded Total RNA Prep with Ribo-Zero Plus (Illumina, USA) following the manufacturer's instructions. Library quality and concentration were evaluated through capillary electrophoresis (Fragment Analyser, AATI) and fluorometry (Qubit 3.0), respectively. Sequencing was performed on a HiSeq2500 (Illumina) using a 100 bp paired-end PE approach.

2.9. RNA-seq data analysis

Removal of reads adapters and quality filtering were performed by TrimGalore (https://github.com/FelixKrueger/TrimGalore). Trimmed reads were mapped to coding regions (CDS) on the genome of *L. monocytogenes* ULE1265 (NCBI GenBank JALDPS000000000), previously extracted by prodigal v2.6.3 (Hyatt et al., 2006), using Bowtie2 c2.3.5.1 (Langmead and Salzberg, 2012) with the -very-sensitive and -end-to-end parameters. Read coverage per CDS from. sam files generated was calculated by using the samtools idxstats command (Danecek et al., 2021). Genes showing differential gene expression (DGE) on planktonic and biofilm samples treated with PAW as compared to the untreated samples were identified with DESeq2 (v 1.30.1) (Love et al., 2014) using DESeq2 R-package. Significance on DGE results was defined by a $\log_2$ fold change >1 and an adjusted p-value (padj) < 0.05. Functionality of DEGs was determined by EggNOG-mapper v2.1.3 (Cantalapiedra et al., 2021) using MMseqs2 (Steinegger and Söding, 2017), which annotates functions according to Clusters of Orthologous Genes (COG), GO, KEGG and PFAM databases. Additionally, the presence of virulence and antimicrobial resistance genes within DEGs was evaluated with a BLAST alignment against the Virulence Finder Database (VFDB) (Chen et al., 2016), ResFinder database (Bortolaia et al., 2020) and Antibacterial Biocide & Metal Resistance Genes Database (BacMet) (Pal et al., 2014), with cut-off values of identity and coverage higher than 99%. Furthermore, some DEGs that did not pass the coverage cut-off value were inspected through blast of the entire genome to the corresponding database or by translation of CDS sequences to proteins, in order to detect incomplete or truncated genes.

2.10. Statistical analysis

Differences in composition (pH values and concentration of nitrates, nitrites and hydrogen peroxide) between the different PAWs tested and tap water were evaluated using analysis of variance (ANOVA) followed by a multiple comparison test using Tukey HSD, considering differences statistically significant at $p < 0.05$. All the analyses were performed with

R Studio version 4.0.4.

3. Results and discussion

3.1. Effect of PAW generation conditions on its physico-chemical properties and the inactivation of L. monocytogenes planktonic cells

The pH value and concentration of nitrites, nitrates and hydrogen peroxide in PAW generated under the different combinations of plasma power and activation time are shown in Table 1. The concentration of all the measured long-lived reactive species increased with plasma power and activation time, with NO_2^- concentrations ranging from 2.1 ± 0.1 to 32.4 ± 5.6 mg/L, NO_3^- concentrations from 75.6 ± 2.3 to 462.3 ± 1.2 mg/L and H_2O_2 concentrations from 0.6 ± 0.1 to 8.8 ± 0.4 mg/L. Acidification of the tap water was observed for all the tested activation conditions but the observed pH decrease was more pronounced at the highest plasma power and longest activation time, with PAW HM30 showing the lowest pH value of 2.3 ± 0.01.

Higher concentration of RONS and more acidic pH in PAW were observed at longer activation time and/or higher plasma power, as previously reported in the literature (Zhao et al., 2020a). It is noteworthy that the operation conditions used in our study were selected based on the trends previously described by Vaka et al. (2019) and Sharmin et al. (2021,b) using the same PAW generation system.

The inactivation efficacy of the different PAWs was screened against the cocktail of three *L. monocytogenes* strains on planktonic state in order to identify the most relevant PAW generation settings for further testing on biofilm cells. The highest antimicrobial activity was also found for PAW HM30, with $\log_{10}$ reductions of 2.2 ± 0.1, 4.6 ± 0.1 and >5.6 (for values below the detection limit of the colony count method, i.e., 10 CFU/mL) after 5, 15 and 30 min of exposure, respectively (Fig. 1). PAW LM30 showed lower antimicrobial activity, resulting in 1.3 ± 0.1, 1.9 ± 0.1 and 3.4 ± 0.2 $\log_{10}$ reductions after 5, 15 and 30 min of exposure, respectively. Almost no inactivation was caused by PAW LM5 as compared to the control treatment with tap water. For *Listeria innocua*, a common surrogate of *L. monocytogenes*, the treatment of planktonic cells for 15 min with PAW generated using a plasma beam system operating at 20 kHz and 5 min of activation time, resulted in 4.9 $\log_{10}$ reductions (Zhao et al., 2021). Similarly, Zhao et al. (2020b) achieved $\log_{10}$ reductions higher than 5.7 after 5 min of cells exposure to PAW generated by 5-min activation using a cold atmospheric plasma jet operating at 20 kHz and 30 kV (Zhao et al., 2020b).

3.2. PAW mode of antimicrobial action

The inactivation results of the exposure of the three *L. monocytogenes* strains cocktail in planktonic state for 30 min to different chemical solutions that partially mimicked the pH and RONS concentration in PAW HM30 are shown in Table 2. While the 30-min PAW treatment led to more than 5.9 $\log_{10}$ reductions, the inactivation achieved with the chemical solutions containing equivalent concentrations of nitrates and nitrites ("NO_2^- + NO_3^-") and hydrogen peroxide ("H_2O_2") but an unadjusted pH higher than 4.5 was limited, with mean $\log_{10}$ reductions of 0.2 ± 0.1 and 0.6 ± 0.2, respectively. Interestingly, the treatment with the chemical solution of nitrates, nitrites, hydrogen peroxide and pH adjusted to 2.3 ("NO_2^- + NO_3^- + H_2O_2 + pH 2.3") resulted in higher inactivation, with mean $\log_{10}$ reduction of 4.8 ± 0.2, but still lower than the inactivation achieved with PAW.

These results are in partial agreement with previous investigations using *Escherichia coli*, where the exposure for 10 min to acidified (pH 3.1) nitrate (2.42 mM), nitrite (~0.38 mM) and hydrogen peroxide (1.20 mM) individual solutions resulted in $\log_{10}$ reductions lower than 1.06 while the treatment with an acidified solution combining the previous RONS led to 3.63 $\log_{10}$ reductions, still lower than the 4.4 $\log_{10}$ reductions achieved by PAW (Zhou et al., 2018). For *Hafnia alvei*, almost no inactivation was found after 30-min treatments with acidified (pH 3.0) nitrate (0.13 mM) and hydrogen peroxide (0.01 mM) individual solutions ($\log_{10}$ reductions lower than 0.5) but higher antimicrobial activities were achieved by the acidified individual nitrite (1.6 mM) solution, which resulted in 3.9 $\log_{10}$ reductions. However, the inactivation achieved with an acidified solution combining the previous RONS (5.7 $\log_{10}$ reductions) was lower than the obtained with PAW (>5.9

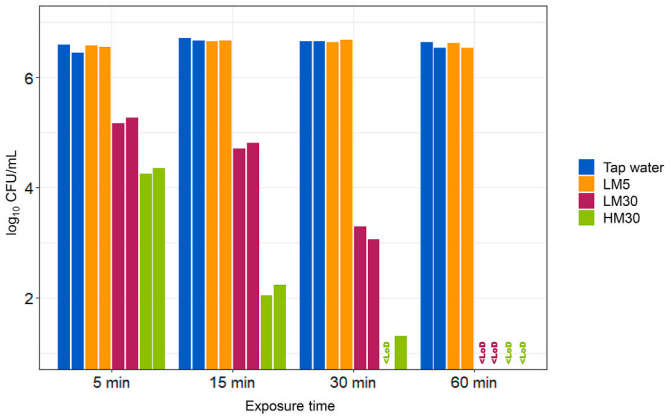

Fig. 1. Inactivation of L. *monocytogenes* planktonic cells by PAW (low mode discharge power and 5 min of activation (LM5) in orange; low mode discharge power and 30 min of activation (LM30) in red; high mode discharge power and 30 min of activation (HM30) in green) and tap water (blue). Total viable counts are expressed as $\log_{10}$ CFU/mL. Duplicates are represented as 2 bars for each condition. <LoD: $\log_{10}$ CFU/mL < 1. (For interpretation of the references to colour in this figure legend, the reader is referred to the Web version of this article.)

Table 1
pH and reactive oxygen and nitrogen species (RONS) concentration in PAW and tap water.

Tap water	NO_2^- (mg/L)	NO_3^- (mg/L)	H_2O_2 (mg/L)	pH
	<LoD	<LoD	<LoD	8.0 ± 0.7
PAW LM5	2.1 ± 0.1[b]	75.6 ± 2.3[c]	0.6 ± 0.1[b]	3.7 ± 0.0[c]
PAW LM30	11.0 ± 5.7[b]	405.1 ± 1.2[b]	8.5 ± 0.3[a]	2.4 ± 0.0[b]
PAW HM30	32.4 ± 5.6[a]	462.3 ± 1.2[a]	8.8 ± 0.4[a]	2.3 ± 0.0[a]

<LoD: below limit of detection.
Different letters indicate a significant difference ($p < 0.05$) among values in the same column.

Table 2
pH, RONS concentration and inactivation ($\log_{10}$ reductions) of the three *L. monocytogenes* strains cocktail on planktonic state upon 30 min exposure to PAW HM30 and to the chemical solutions that partially mimic PAW HM30.

PAW/ Chemical solution	NO_2^-(mg/L)	NO_3^-(mg/L)	H_2O_2 (mg/L)	pH	$\log_{10}$ reductions
PAW HM30	32.4	462.3	8.8	2.3	>5.88
pH 2.3	–	–	–	2.3 (adjusted)	3.9
NO_2^- + NO_3^-	32.4	462.3	–	6.3 (no adjusted)	0.2
H_2O_2	–	–	8.8	4.5 (no adjusted)	0.6
NO_2^- + NO_3^- + H_2O_2 + pH 2.3	32.4	462.3	8.8	2.3 (adjusted)	4.8

$\log_{10}$ reductions) (Naítali et al., 2010).

In our case, the 30-min exposure of *L. monocytogenes* planktonic cells to the solution that mimicked PAW HM30 pH (~2.3) but with no nitrites, nitrates or hydrogen peroxide, resulted in 3.9 ± 0.1 $\log_{10}$ reductions, which is higher than the inactivation described in the literature for acid water solutions mimicking PAW pH. However, the PAWs used on those previous studies presented higher pH values, of approximately 3.0, and other microorganisms rather than *L. monocytogenes* were tested (Naítali et al., 2010; Zhou et al., 2018). Even though there is little information regarding *L. monocytogenes* inactivation in the range of pH below 3, $\log_{10}$ reductions in the range of 0.5–2.5 have been described for this microorganism exposed to pH 2.7 for 30 min, with a great influence of the *L. monocytogenes* strain being tested (Karatzas et al., 2012).

The results suggested that the antimicrobial activity of PAW involves not only the low pH and RONS considered in this study (NO_2^-, NO_3^-, H_2O_2) but also other non-measured reactive species, such as the superoxide anion ($O_2^{\bullet-}$), hydroxyl radical (•OH), singlet oxygen ($^1O_2$), nitric oxide (NO•), peroxinitrite ($ONOO^-$), etc. (López et al., 2019), since the inactivation values achieved with the chemical solutions that mimicked PAW HM30 were always lower than the $\log_{10}$ reductions obtained with PAW HM30.

3.3. Antimicrobial efficacy of PAW against L. monocytogenes biofilms on SS and polystyrene

The inactivation efficacy of PAW HM30 against *L. monocytogenes* biofilms on stainless steel and polystyrene at different exposure times is shown in Fig. 2. Biofilm formation by the three *L. monocytogenes* strains cocktail after 6 days at 12 °C was slightly higher on polystyrene than on stainless steel, achieving, respectively, 6.6 ± 0.2 and 5.9 ± 0.2 $\log_{10}$ CFU/cm^2. In general, the antimicrobial activity observed on biofilms was lower than that in planktonic state, with $\log_{10}$ reductions after 15 and 30 min of exposure of 1.9 ± 0.1 and 4.5 ± 0.4, respectively, on polystyrene, and 1.8 ± 0.2 and 4.4 ± 0.1, respectively, on stainless steel. At the longest exposure time tested for biofilms (60 min), reductions to levels below the detection limit of the plate counting method (i.e., $\log_{10}$ 1.0 CFU/cm^2) were achieved on stainless steel while 5.4 ± 0.8 $\log_{10}$ reductions were observed on polystyrene.

The effect of PAW exposure time on viable counts of *L. monocytogenes* biofilms was fit to log-linear inactivation kinetics, resulting in *D*-values of 11.3 and 11.2 min for the biofilms formed on stainless steel and polystyrene, respectively, which shows that PAW was similarly effective to remove biofilms formed on both surfaces.

Accordingly, other studies have also shown the effectiveness of PAW in biofilm removal. For example, Handorf et al. (2021) treated biofilms of *L. monocytogenes* on PET-G with PAW generated by microwave induced plasma with a forward power of 80 W and a reverse power of 20 W for 2 min obtaining 4.7 $\log_{10}$ reductions after a 3-min exposure. However, lower PAW inactivation efficacy on biofilms has often been reported as compared to planktonic cells (Mai-Prochnow et al., 2021; Smet et al., 2019). Smet et al. (2019) reported ~ 5.5 $\log_{10}$ reductions after a 15-min PAW exposure for *L. monocytogenes* on planktonic state, but only 3.0 $\log_{10}$ reductions with the same treatment against *L. monocytogenes* biofilms, when using PAW generated for 30 min with a DBD plasma system operating at 15 kHz and 8 kV and with a mixture of helium and 1% (v/v) oxygen as precursor gas.

3.4. Changes in L. monocytogenes gene expression in response to PAW treatment

The transcriptomic response of PAW-treated cells, both on planktonic state and within biofilms, was studied through RNA-seq for a treatment with PAW HM30 able to produce approximately 1 $\log_{10}$ reduction in *L. monocytogenes* ULE1265, i.e. 5 and 15 min of exposure time for planktonic and biofilm cells, respectively (Fig. S1). This L. *monocytogenes* strain was selected for the RNA-seq analyses due to its higher resistance to PAW, as compared to the other two *L. monocytogenes* strains included in this study (Fig. S2), and its persistent nature in the meat industry where it was isolated from. The RNA-seq analysis identified 399 differentially expressed genes (DEGs) as a result of the treatment of *L. monocytogenes* ULE1265 planktonic cells with PAW HM30, 178 of them upregulated and 221 downregulated. Only 8 DEGs, all of them upregulated, were identified for *L. monocytogenes* ULE1265 biofilm cells treated with PAW HM30 (Fig. 3). Even though the fold changes in expression of the DEGs in treated biofilm cells was in general higher than those observed for PAW-treated cells in planktonic state, for the former ones the differences were statistically significant only in a very low

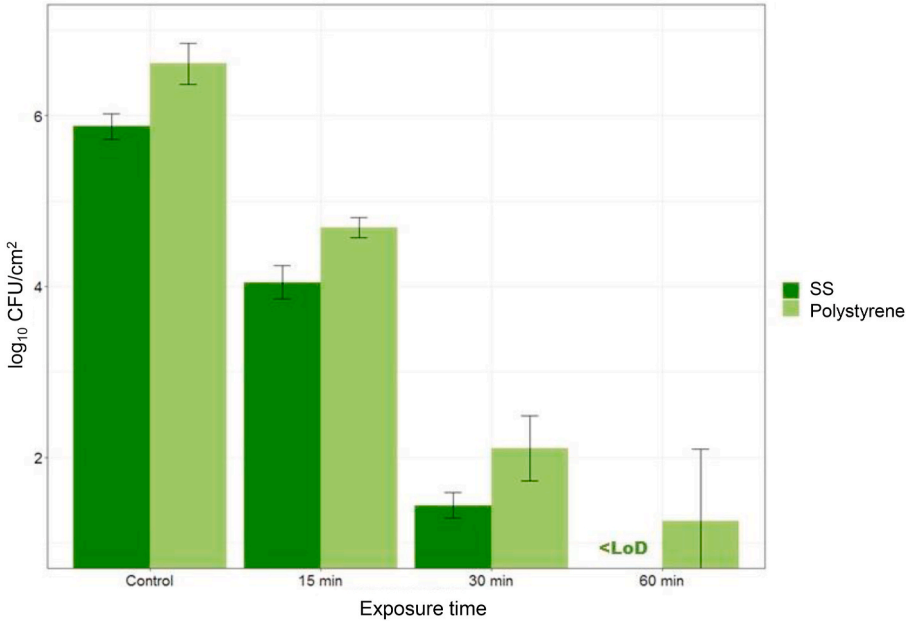

Fig. 2. Inactivation by PAW HM30 of *L. monocytogenes* biofilms formed on SS and on polystyrene. Total viable counts recovered from the PAW-treated and untreated (Control) biofilms are expressed as $\log_{10}$ CFU/cm^2. Error bars represent the standard deviation. <LoD: $\log_{10}$ CFU/cm^2 < 1.02.

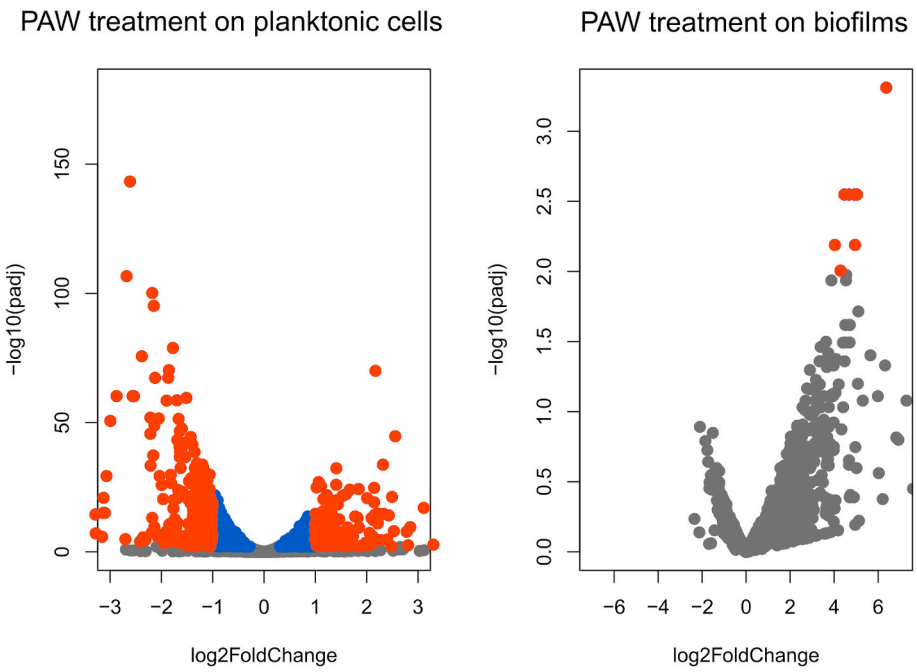

Fig. 3. Volcano plot showing the RNA-seq data analysis of *L. monocytogenes* ULE1265 planktonic (left panel) and biofilm (right panel) cells exposed to PAW for 5 and 15 min, respectively. Grey dots represent all the identified genes, blue dots genes that presented an adjusted p-value (padj) > 0.05, indicating statistically significant differences in gene expression, but with an absolute $\log_2$ fold change lower than 1, and red dots genes that presented an adjusted p-value (padj) > 0.05 and an absolute $\log_2$ fold change higher than 1, which are identified as differentially expressed genes (DEGs). (For interpretation of the references to colour in this figure legend, the reader is referred to the Web version of this article.)

number of genes due to the high variability observed between replicates (Fig. S3).

A principal component analysis (PCA), shown in Fig. 4, evidenced that the gene expression patterns observed for the planktonic cell replicates, both treated with PAW and control, were much more similar among themselves than those for the biofilm cell replicates, especially in the case of PAW-treated biofilms. This high variability between replicates among the biofilm samples made it difficult to study the effect of

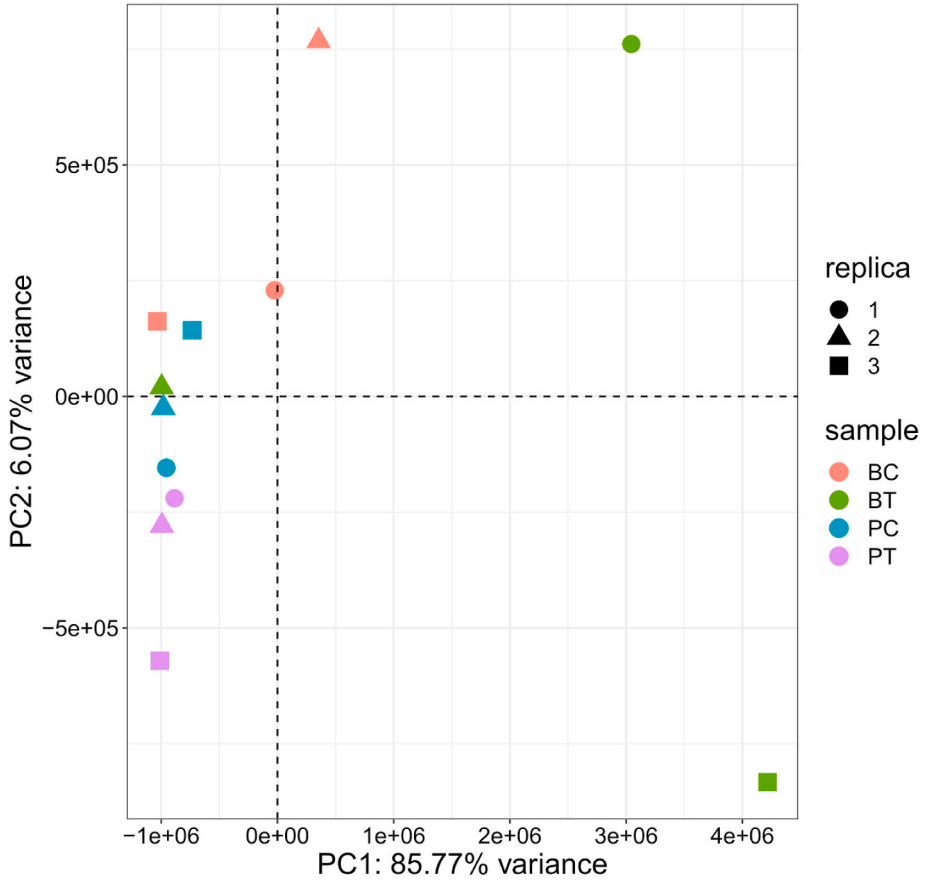

Fig. 4. Principal Component Analysis (PCA) plot of RNA-seq read counts in the three replicas of untreated (PC) and PAW-treated (PT) planktonic cells and untreated (BC) and PAW-treated (BT) biofilm cells.

PAW on the transcriptome of *L. monocytogenes* biofilm cells. RNA-seq is a powerful tool to explore gene expression on homogeneous bacterial populations, such as planktonic cultures, but presents some limitations regarding heterogeneous multicellular systems since it does not preserve the spatial context of the analysis (Evans et al., 2020; Dar et al., 2021). This fact together with the experimental variability associated with biofilm development, cell recovery and RNA extraction might be the reason for the high variability in biofilm RNA-seq results observed in the current study.

The transcriptomic response to PAW treatment was quite different on planktonic and biofilm cells since only two common DEGs were identified (Fig. 5), with both of them being upregulated genes (Table 3). One of them had an unknown function and the other was identified as the gene *cbiH*, included in the well conserved *L. monocytogenes* cobalamin-dependent gene cluster (Anast et al., 2020).

Regarding the transcriptomic response of PAW-treated *L. monocytogenes* planktonic cells (Table 3), the most upregulated genes after the treatment included genes related to cobalamin metabolism, *cbiD* and *cbiH* (Anast et al., 2020), and to ethanolamine metabolism, *eutB* and *eutL* (Mellin et al., 2014). On the other hand, some of the most downregulated genes on the PAW-treated planktonic cells were *bglX-2*, related to starch and sucrose metabolism (Abdelhamed et al., 2020), *yvlC*, a SigB-regulated gene (Chatterjee et al., 2006), and *pstC*, involved in a high affinity phosphate transport system (Moreno-Letelier et al., 2011).

The most affected biological functions by the PAW treatment on planktonic cells, according to COG categorization (Fig. 6), were translation and ribosomal structure (J), carbohydrate transport and metabolism (G) and inorganic ion transport and metabolism (P). Other frequently affected functions were energy production and conversion (C), cell wall/membrane/envelope biogenesis (M) and DNA replication and repair (L). Notably, genes associated with translation and ribosomal structure (J) functions were more frequently found as upregulated DEGs than as downregulated DEGs, while the opposite was found for genes related to carbohydrate transport and metabolism (G) functions. The COG function of cell motility (N) was only represented among upregulated DEGs. Also, 134 out of the 398 DEGs for PAW-treated planktonic cells and 5 out of the 8 DEGs for PAW-treated biofilm cells were classified as associated with an unknown function.

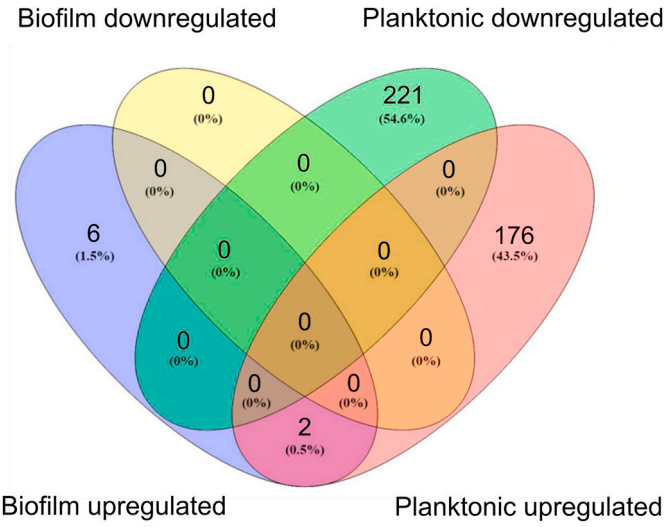

Fig. 5. Venn diagram of differentially expressed genes (DEGs) in response to PAW treatment with circles indicating unique and common up-regulated (red) and down-regulated (green) genes on planktonic state and up-regulated (blue) and down-regulated (yellow) genes on biofilm state. (For interpretation of the references to colour in this figure legend, the reader is referred to the Web version of this article.)

Table 3
Top differentially expressed genes (log_2 fold change >2.5) in response to PAW treatment.

		log_2 fold change	padj	gene	COG category
Planktonic	Upregulated	3.79	6.00E-04	*cbiD*	H
		3.30	1.73E-03	*cbiH* *	H
		3.11	1.03E-17	*eutC*	E
		2.85	2.80E-10	*eutB*	E
		2.81	2.80E-03	-	V
		2.78	1.65E-08	*eutL*	E
		2.56	1.94E-45	-	–
		2.53	9.79E-09	-	–
	Downregulated	−4.74	1.73E-13	-	G
		−3.49	1.95E-25	*bglX-2*	G
		−3.41	2.67E-180	*yvlC*	KT
		−3.29	3.45E-15	-	G
		−3.28	7.28E-08	-	G
		−3.15	1.50E-06	-	G
		−3.13	9.04E-16	*pstC*	P
		−3.13	1.29E-21	-	G
		−3.10	9.41E-16	-	G
		−3.07	4.80E-30	-	G
		−2.99	2.21E-51	-	G
		−2.87	5.55E-61	*adhE/lap*	C
		−2.70	1.28E-05	-	S
		−2.68	2.31E-107	-	C
		−2.61	5.22E-144	*telA1*	P
		−2.56	5.55E-61	-	G
		−2.53	6.28E-61	*menG*	H
Biofilm	Upregulated	6.37	4.89E-04	*cbiH* *	H
		5.03	2.83E-03	-	S
		4.95	6.48E-03	-	S
		4.92	2.83E-03	*bcrB*	–
		4.68	2.83E-03	*cheR*	NT
		4.46	2.83E-03	-	S
		4.29	9.88E-03	-	G
		4.03	6.48E-03	-	–

H: Coenzyme transport and metabolism, E: Amino acid transport and metabolism, V: Defense mechanisms, G: Carbohydrate transport and metabolism, K: Transcription, T: Signal transduction mechanisms, P: Inorganic iron transport and metabolism, S: Function unknown, N: Cell motility.
* Upregulated gene in both planktonic and biofilm cells.
padj: adjusted p-value.

COG: Clusters of Orthologous Genes.
-: no information available in the database.

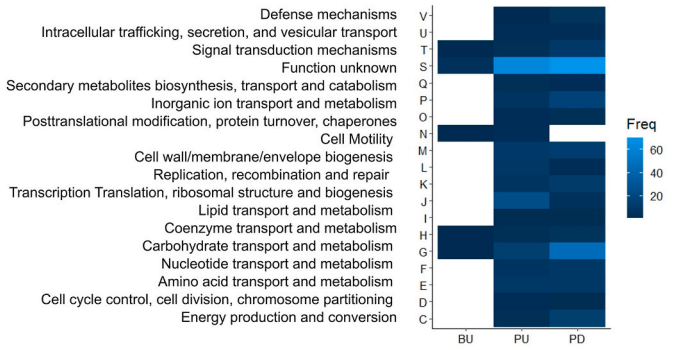

Fig. 6. Heatmap representing the number of differentially expressed genes (DEGs) upregulated on PAW-treated biofilm cells (BU) and PAW-treated planktonic cells (PU) and DEGs downregulated on PAW-treated planktonic cells (PD) assigned to different Clusters of Orthologous Genes (COG) categories.

In general, PAW treatment induced profound changes in carbon metabolism, with a 7.3% of the upregulated genes and a 20.8% of the downregulated genes in planktonic cells being associated with carbohydrate transport and metabolism functions according to COG categorization. In fact, as previously mentioned, one of the most downregulated genes was *bglX-2*, a beta-glucosidase involved in starch and sucrose metabolism. In many bacteria, including *L. monocytogenes*, carbohydrates are transported mainly by specific phosphoenolpyruvate (PEP)-dependent phosphotransferase systems (PTSs) (Stoll and Goebel, 2010). Some of the DEGs belonged to PTSs (Table 4), where a downregulation of genes related to the cellobiose, galactitol and fructose PTSs and an upregulation of genes related to sorbitol, β-glucoside and mannose PTSs was observed (Fig. S4). A downregulation of *manR*, the transcriptional activator of some genes from the PTS Man, Lac and Gut families (Stoll and Goebel, 2010), was also observed. The few published studies on cold plasma mechanisms of inactivation using transcriptomic approaches are focused on differential expression of stress, quorum sensing and virulence related genes but not on changes in carbon metabolism related functions. However, the transcriptomic response to low pH, a major characteristic of PAW, has been previously investigated in more detail. For example, Horlbog et al. (2019) observed an upregulation of PTSs, including fructose, mannose, galacitol and lactose PTSs, and the regulator of the cellobiose PTS (*licR*), after the exposure of planktonic cells of acid-resistant *L. monocytogenes* strains to HCl at pH 3.0 for 1 h, results that differed from metabolic changes observed in the current study. Additionally, Horlbog et al. (2019) found an upregulation of all components of the non-PTS glycerol catabolism pathway, while our results showed a downregulation of the genes *glpK* and *glpD*, involved in the conversion of glycerol into dihydroxyacetone (Koomen et al., 2018).

An induction of the cobalamin-dependent gene cluster (CDGC), responsible for the catabolism of ethanolamine and 1,2-propanediol, was observed (Table 4). Multiple genes belonging to the CDGC (*cbiD*, *cbiH*, *eutB*, *eutC*, *eutE*, *eutH*, *eutL*, *eutT* and *pduX*) were upregulated after the PAW treatment on planktonic cells, some of them being among the most upregulated ones (log_2 fold change >2.5), and the *cbiH* gene was also upregulated on PAW-treated biofilms. The CDGC cluster is large, including the *eut*, *pdu*, and *cob/cbi* operons, well conserved in *L. monocytogenes* and that might have been acquired by lateral gene transfer in an ancestor according to genome-level evolutionary studies (Buchrieser et al., 2003; Chiara et al., 2015; Shelton et al., 2019). The *eut* operon is involved in the utilization of ethanolamine as a carbon and nitrogen source and the *pdu* operon participates in the metabolism of 1, 2-propanediol. The enzymes involved in those pathways are dependent

Table 4
Genes involved in metabolism, stress response and virulence of *L. monocytogenes* showing a differential expression in planktonic cells exposed to PAW.

	log_2 fold change	padj	gene	COG category	putative funtion
Upregulated	2.17	9.61E-71	*manX/manL*	G	PTS
	1.47	4.71E-04	*bglF*	G	
	1.31	4.48E-03	*srlB*	G	
	1.98	2.80E-04	*eutT*	E	CDGC
	1.85	4.44E-10	*eutE*	C	
	1.57	3.01E-03	*pduX*	Q	
	1.13	4.09E-03	*eutH*	E	
	1.60	7.27E-03	*gadC*	E	SigmaB regulated
	1.12	7.54E-14	*Eno*	F	
	1.11	9.15E-08	*clpP*	OU	
	1.11	1.12E-15	*Pgk*	F	
	1.03	1.23E-25	*cggR*	K	
	1.29	5.52E-20	*agrB*	KOT	Quorum sensing
	1.73	8.87E-07	*fliH*	G	Virulence
	1.67	9.63E-25	*flgE*	M	
	1.31	3.02E-13	*inlA*	K	
	1.24	8.83E-04	*fliI*	S	
	1.13	3.48E-10	*Iap*	MT	
	1.10	2.74E-04	*lmo0685/ywaC*	S	
	1.24	7.56E-10	*accB*	I	Fatty acid biosynthesis
	1.06	1.05E-04	*fabI*	I	
	1.41	4.96E-33	*mntB*	P	Manganese transport
	1.09	4.84E-07	*mntR*	K	
	1.78	2.23E-14	*ebrA*	U	Plasmid-encoded
	1.63	4.46E-08	*qacC*	U	
	1.47	1.81E-06	*tnpR*	L	
Downregulated	−2.38	2.19E-76	*celA/chbB*	G	PTS
	−2.31	2.19E-05	*manY*	G	
	−1.97	3.99E-21	*lmo029*	G	
	−1.97	3.99E-21	*lmo0299*	G	
	−1.82	1.67E-30	*gatC/sgcC*	G	
	−1.80	1.05E-08	*celC/chbA/ptcA*	G	
	−1.77	1.65E-17	*gatB/sgcB*	G	
	−1.28	1.29E-10	*gatA/sgcA*	G	
	−1.23	1.90E-19	*manR*	G	
	−1.12	8.38E-04	*celB/chbC*	G	

(*continued on next page*)

Table 4 (*continued*)

	log_2 fold change	padj	gene	COG category	putative funtion
	−1.09	5.10E-06	*fruA*	G	
	−1.46	3.06E-13	*bglF/bglP*	G	
	−1.21	9.85E-21	*glpD*	C	Glycerol metabolism
	−1.10	1.61E-28	*glpK*	F	
	−1.61	3.18E-40	*clpC*	O	SigmaB regulated
	−1.17	1.28E-23	*dtpT*	P	
	−1.03	5.09E-12	*phoU*	P	
	−1.00	2.17E-19	*Ldh*	C	
Downregulated	−1.36	6.32E-05	*actA*	S	Virulence
	−1.61	3.18E-40	*clpC*	O	
	−1.33	7.48E-03	*clpE*	O	
	−1.27	4.84E-24	*fliD*	T	
	−2.03	4.67E-30	*Hly*	M	
	−1.08	9.28E-23	*lap/rnjB*	J	
	−1.39	5.59E-13	*lspA/arpJ*	P	
	−1.63	7.66E-07	*plcA*	U	
	−2.35	2.51E-06	*plcB*	M	

M: Cell wall/membrane/envelope biogenesis, T: Signal transduction mechanisms, O: Posttranslational modification, protein turnover, chaperones, U: Intracellular trafficking, secretion, and vesicular transport, I: Lipid transport and metabolism, E: Amino acid transport and metabolism, K: Transcription, L: Replication, recombination and repair, F: Nucleotide transport and metabolism, S: Function unknown, G: Carbohydrate transport and metabolism, C: Energy production and conversion, P: Inorganic ion transport and metabolism, J: Translation, ribosomal structure and biogenesis, H: Coenzyme transport and metabolism.
padj: adjusted p-value.
COG: Clusters of Orthologous Genes.
PTS: Phosphoenolpyruvate-dependent Phosphotransferase Systems.
CDGC: Cobalamin-Dependent Gene Cluster.

on cofactors derived from cobalamin (vitamin B_{12}), which is synthesized *de novo* via the *cob* and *cbi* genes (Anast et al., 2020). The CDGC has been associated with pathogenicity in many enteric pathogens and, in *L. monocytogenes*, the upregulation of this cluster, together with the galactitol, fructose, and cellobiose uptake PTSs and glycerol utilization genes, has been described as a metabolic adaptation to the intestinal tract and blood (Anast et al., 2020; Fuchs et al., 2012). The activation of the CDGC may increase competitive fitness over commensal bacteria in the gastrointestinal tract but also in other environments since an induction of the CDGC has been also observed in *L. monocytogenes* after co-cultivation with *Bacillus subtilis*, *Carnobacterium*, *Lactobacillus*, *Psychrobacter* and *Brevibacterium* (Anast and Schmitz-Esser, 2020). The importance of *L. monocytogenes* CDGC in the response to food production associated stresses, such as cold temperatures, disinfectants, acidic conditions and desiccation, has been already described but the knowledge regarding the specific mechanisms is still limited (Anast et al., 2020).

L. monocytogenes gene expression under stress conditions is controlled by multiple transcriptional regulators, with the alternative sigma factor SigB, σ^B, controlling the largest regulon and being currently considered the master regulator of the general stress response, virulence and resilience (Alvarez-Ordóñez et al., 2015; Liu et al., 2019). In the current study, several genes from the σ^B regulon were identified among the DEGs (Table 4), both upregulated (*cggR*, *pgk*, *eno*, *gadC*, *clpP*) and downregulated (*ldh*, *clpC*, *dtpT*, *phoU*). The ATP-dependent proteases encoded by *clpP* and *clpC* belong to the CtsR regulon, involved in the response to various stressors and in virulence (Chatterjee et al., 2006; Liu et al., 2019), and c*ggR* is the central glycolytic regulator (Liu et al., 2019). Interestingly, the upregulated gene *gadC* encodes one of the components of the glutamate decarboxylase (GAD) system, one of the principal systems involved in *L. monocytogenes* acid stress response (Arcari et al., 2020). The induction of the GAD system can be easily directly linked to the low pH (2.33 ± 0.01) of the PAW used. In fact, an upregulation of the GAD system has been observed after the treatment of *L. monocytogenes* with HCl at pH 3.0 (Horlbog et al., 2019) and lactic acid at pH 3.4 (Cortes et al., 2020), as well as following a treatment with atmospheric cold plasma (Patange et al., 2019).

Previous available studies that analysed the effect of a direct cold plasma treatment on *L. monocytogenes* gene expression using RT-PCR focused on the impact on genes related to the σ^B regulon, virulence, quorum-sensing and the GAD system (Cui et al., 2021; Patange et al., 2019). Patange et al. (2019) observed on *L. monocytogenes* plasma-treated planktonic cells, not only the previously mentioned upregulation of the GAD system, but also an activation of the σ^B regulon, via the positive regulators *sigB* and *rsbR*, and an upregulation of the *prfA* gene, that positively regulates the expression of *L. monocytogenes* virulence genes. On L. *monocytogenes* biofilms treated with cold nitrogen plasma, Cui et al. (2021) described an upregulation of *sigB*, a downregulation of virulence related genes, including the regulator *prfA*, and a variable regulation of quorum-sensing related genes. In the present study, although some σ^B- regulated genes were differentially expressed (Table 4), no differences in *sigB* and *rsbR* expression were observed. Similarly, some virulence-related genes were differentially expressed (Table 4) but the expression of the virulence regulator *prfA* was not affected by the PAW treatment. Regarding quorum sensing-related gene expression (Table 4), the PAW treatment produced an upregulation of *agrB*, which belongs to the *agr* operon, involved in the regulation of virulence and in the initial adhesion phase of biofilm formation (Gandra et al., 2019; Garmyn et al., 2012; Zetzmann et al., 2019).

A BLAST alignment of the DEGs against virulence and antimicrobial resistance gene databases allowed the identification of one upregulated gene on the PAW-treated biofilm cells (Table 3), *bcrB*, involved in resistance to quaternary ammonium compounds, and 8 DEGs on the PAW-treated planktonic cells (Table 4), both upregulated (*fliE*, *fliH*, *fliI*, *motA*, *inlA*) and downregulated (*fliD*, *lap*, *lspA*), related to virulence. Interestingly, two of those genes, *bcrB* and *inlA*, presented premature stop codons that could lead to truncated non-functional proteins.

The combination of the previously described BLAST alignment and the initial gene functionality assignment resulted in the identification of several DEGs, for PAW-treated planktonic cells, associated with virulence (Table 4), including both upregulated (*clpP*, *fliE*, *fliH*, *fliI*, *iap*, *inlA* and *lmo0685*) and downregulated (*actA*, *clpC*, *clpE*, *fliD*, *hly*, *lap*, *lspA*, *plcA* and *plcB*) genes. While studies investigating the effect of cold plasma on *L. monocytogenes* (Cui et al., 2021; Patange et al., 2019) and PAW on *Enterococcus faecalis* (Li et al., 2019) showed a downregulation of virulence genes as a result of these treatments, studies of *L. monocytogenes* exposure to low pH, a major characteristic of PAW, showed an upregulation of virulence related genes (Cortes et al., 2020; Horlbog et al., 2019). Most of the virulence related upregulated genes in the current study (*fliE*, *fliH*, *fliI*, *motA*) are involved in flagellar biosynthesis and motor control which, in combination with the upregulation of the chemotaxis signalling cascade gene *cheR* on PAW-treated biofilms, might indicate an increase in bacterial motility in order to avoid the unfavourable environment (Casey et al., 2014). Additionally, flagellar motility has been previously shown to play an important role on initial surface attachment and subsequent biofilm formation of

L. monocytogenes (Lemon et al., 2007). In spatially organized bacterial communities such as biofilms, the environmental variations can transform colony morphology by chemotactic motility due to cell migration towards more favourable places (Tasaki et al., 2017). It is important to mention that one of the upregulated virulence genes, *inlA*, involved on cell invasion, presented a loss-of-function mutation that results in a truncated version of the Internalin A (InlA) protein. This type of *inlA* mutations have been associated with a hypovirulent phenotype, which is more common on *L. monocytogenes* isolates from foods and food processing environments (Alvarez-Molina et al., 2021; Ferreira da Silva et al., 2017).

It is considered that microbial inactivation upon exposure to PAW starts when the coexistence of RONS and low pH values causes physical and oxidative stress to the cells, which results in a compromised membrane integrity that facilitates the import of RONS and protons to the intracellular environment and leads to DNA, protein, lipid and carbohydrate oxidation (Mai-Prochnow et al., 2021; Zhao et al., 2020b). Therefore, the presence of DEGs related to oxidative stress and the repair of membrane and DNA damage after the PAW treatment was also evaluated. As indicated in Table 4, PAW-treated cells showed an upregulation of genes involved in fatty acids biosynthesis (*accB*, *fabI*), which has been previously observed on *L. monocytogenes* cells treated with benzethonium chloride, a biocide that causes the solubilisation of the hydrophobic components in the cell membrane (Casey et al., 2014). However, almost no DEGs related to the oxidative stress response were identified (Huang et al., 2018; Seixas et al., 2022), only the upregulation of the genes *mntB* and *mntR*, involved in the transport of manganese, which is a co-factor for superoxide dismutase (Cortes et al., 2020; Kragh and Truelstrup Hansen, 2020). Also, no activation of the SOS response, involved in DNA repair, was detected (van der Veen et al., 2010).

The L.*monocytogenes* strain ULE1265 contains a plasmid that has been previously characterized in detail (Alvarez-Molina et al., 2021). The PAW treatment of planktonic cells resulted in an upregulation of the plasmid-encoded genes *tnpR*, *qacC* and *ebrA* (Table 4), the last two being putative multidrug exporters. On PAW-treated biofilms, an upregulation of the plasmid-encoded gene *bcrB* was observed (Table 3). This gene is part of the cassette *bcrABC*, responsible for benzalkonium chloride tolerance and often described as plasmid-associated. However, this gene presented a premature stop codon that could lead to a truncated and likely non-functional protein.

4. Conclusions

In the current study, a direct relationship between PAW generation parameters (plasma power and activation time) and PAW composition and antimicrobial activity has been observed, with lower pH and higher RONS concentration and antilisterial activity being achieved upon the most extreme PAW generation conditions (36 W plasma power and 30 min activation time). The influence of the cell arrangement as planktonic or biofilm cells on the inactivation efficacy of PAW was demonstrated on a three *L. monocytogenes* strains cocktail. Thus, a 15-min PAW treatment resulted in 4.6 $\log_{10}$ reductions for planktonic cells but only 1.9 and 1.8 $\log_{10}$ reductions for biofilms formed on polystyrene and SS, respectively. However, an increased PAW exposure time of 60 min led to $>$5.4 $\log_{10}$ reductions for *L. monocytogenes* biofilms grown on SS. The treatment of *L. monocytogenes* planktonic cells with solutions that partially mimicked the pH and nitrate, nitrite and hydrogen peroxide concentration in PAW HM30 suggested an additive antimicrobial effect of RONS and pH, with an important role of the acidic pH. A transcriptomic analysis of the response of *L. monocytogenes* ULE1265 to PAW showed a general remodelling of carbon metabolism, with differential expression of many PTSs, and a strong upregulation of the cobalamin-dependent gene cluster (CDGC), involved on ethanolamine and 1,2-propanediol metabolism. The treatment of planktonic cells with PAW affected the expression (either up- and down-regulation) of some genes related to virulence and to the general stress response, controlled by the alternative sigma factor SigB. Also, an upregulation of the GAD system, involved in the acid stress response, was observed, but no relevant changes in the expression of components of the oxidative stress response were detected under the tested conditions. Overall, the present study has demonstrated the potential of PAW as an effective alternative to conventional chemical disinfectants used in the food industry, and has contributed to an improved understanding of PAW's mode of antimicrobial action.

Disclaimer

The author, Estefanía Noriega Fernández, is employed with the European Food Safety Authority (EFSA) at the Nutrition Unit that provides scientific and administrative support to the Panel on "Nutrition, Novel Foods and Food Allergens" in the area "Safety Assessment of Novel Foods". However, the present article is published under the sole responsibility of the authors Paula Fernández-Gómez, José F. Cobo-Díaz, Marcia Oliveira, Montserrat González-Raurich, Avelino Alvarez-Ordóñez, Miguel Prieto, James L. Walsh, Morten Sivertsvik, Estefanía Noriega-Fernández, Mercedes López and may not be considered as an EFSA scientific output. The positions and opinions presented in this article are those of the author/s alone and are not intended to represent the views/any official position or scientific works of EFSA. For more information about the views or scientific outputs of EFSA, please consult its website under http://efsa.europa.eu.

Declaration of competing interest

The authors declare no conflict of interest.

Acknowledgements

This work was supported by the Research Council of Norway (iNO-Box 281106), the COST Action CA18113 (EuroMicropH) and the Spanish Ministry of Science and Innovation (MICINN) State Plan for Scientific and Technical Research and Innovation 2017–2020 [PID 2020-113658RB-C22]. The author P. Fernández-Gómez is grateful to Junta de Castilla y León and the European Social Fund (ESF) for awarding her a pre-doctoral grant [BOCYL-D-15122017-4]. The author M. Oliveira is in receipt of a Juan de la Cierva - Incorporación contract [IJC 2018-035523 I] awarded by the Spanish Ministry of Science and Innovation (MCIN/AEI/10.13039/501100011033).Library preparation and sequencing for RNA-seq was performed by the sequencing platform of *Centro de Investigación Biomédica de La Rioja* (CIBIR), Spain.

Appendix A. Supplementary data

Supplementary data to this article can be found online at https://doi.org/10.1016/j.fm.2023.104252.

References

Abdelhamed, H., Ramachandran, R., Narayanan, L., Ozdemir, O., Cooper, A., Olivier, A. K., Karsi, A., Lawrence, M.L., 2020. Contributions of a LysR transcriptional regulator to *Listeria monocytogenes* virulence and identification of its regulons. J. Bacteriol. 202 (10), 1–19. https://doi.org/10.1128/JB.00087-20.

Alvarez-Molina, A., Cobo-Díaz, J.F., López, M., Prieto, M., de Toro, M., Alvarez-Ordóñez, A., 2021. Unraveling the emergence and population diversity of *Listeria monocytogenes* in a newly built meat facility through whole genome sequencing. Int. J. Food Microbiol. 340 (December 2020) https://doi.org/10.1016/j.ijfoodmicro.2021.109043.

Alvarez-Ordóñez, A., Broussolle, V., Colin, P., Nguyen-The, C., Prieto, M., 2015. The adaptive response of bacterial food-borne pathogens in the environment, host and food: implications for food safety. Int. J. Food Microbiol. 213, 99–109. https://doi.org/10.1016/j.ijfoodmicro.2015.06.004.

Alvarez-Ordóñez, A., Coughlan, L.M., Briandet, R., Cotter, P.D., 2019. Biofilms in food processing environments: challenges and opportunities. Annu. Rev. Food Sci. Technol. 25 (10), 173–195. https://doi.org/10.1146/annurev-food-032818-121805.

Anast, J.M., Bobik, T.A., Schmitz-Esser, S., 2020. The Cobalamin-Dependent Gene Cluster of *Listeria monocytogenes*: implications for virulence, stress response, and food

safety. Front. Microbiol. 11 (November), 1–9. https://doi.org/10.3389/fmicb.2020.601816.
Anast, J.M., Schmitz-Esser, S., 2020. The transcriptome of *Listeria monocytogenes* during co-cultivation with cheese rind bacteria suggests adaptation by induction of ethanolamine and 1,2-propanediol catabolism pathway genes. PLoS One 15 (7 July), 1–26. https://doi.org/10.1371/journal.pone.0233945.
Arcari, T., Marie-Lucie, F., Guerreiro, D.N., Wu, J., Conor, P.O., 2020. Comparative review of the responses of *Listeria monocytogenes* and *Escherichia coli* to low pH stress. Genes 11, 1330. https://doi.org/10.3390/genes11111330.
Baek, K.H., Yong, H.I., Yoo, J.H., Kim, J.W., Byeon, Y.S., Lim, J., Yoon, S.Y., Ryu, S., Jo, C., 2019. Antimicrobial effects and mechanism of plasma activated fine droplets produced from arc discharge plasma on planktonic *Listeria monocytogenes* and *Escherichia coli* O157:H7. Mater. Res. Express 6 (12), 125337.
Bortolaia, V., Kaas, R.S., Ruppe, E., Roberts, M.C., Schwarz, S., Cattoir, V., Philippon, A., Allesoe, R.L., Rebelo, A.R., Florensa, A.F., Fagelhauer, L., Chakraborty, T., Neumann, B., Werner, G., Bender, J.K., Stingl, K., Nguyen, M., Coppens, J., Xavier, B. B., et al., 2020. ResFinder 4.0 for predictions of phenotypes from genotypes. J. Antimicrob. Chemother. 75 (12), 3491–3500. https://doi.org/10.1093/jac/dkaa345.
Bridier, A., Sanchez-Vizuete, P., Guilbaud, M., Piard, J.C., Naïtali, M., Briandet, R., 2015. Biofilm-associated persistence of food-borne pathogens. Food Microbiol. 45 (PtB), 167–178. https://doi.org/10.1016/j.fm.2014.04.015.
Buchrieser, C., Rusniok, C., Kunst, F., Cossart, P., Glaser, P., Frangeul, L., Amend, A., Baquero, F., Berche, P., Bloecker, H., Brandt, P., Chakaborty, T., Charbit, A., Chétouani, F., Couvé, E., De Daruvar, A., Dehoux, P., Domann, E., Domínguez-Bernal, G., et al., 2003. Comparison of the genome sequences of *Listeria monocytogenes* and *Listeria innocua*: clues for evolution and pathogenicity. FEMS Immunol. Med. Microbiol. 35 (3), 207–213. https://doi.org/10.1016/S0928-8244(02)00448-0.
Cantalapiedra, C.P., Hernández-Plaza, A., Letunic, I., Bork, P., Huerta-Cepas, J., 2021. eggNOG-mapper v2: functional annotation, orthology assignments, and domain prediction at the metagenomic scale. Mol. Biol. Evol. 38 (12), 5825–5829. https://doi.org/10.1093/molbev/msab293.
Casey, A., Fox, E.M., Schmitz-Esser, S., Coffey, A., McAuliffe, O., Jordan, K., 2014. Transcriptome analysis of *Listeria monocytogenes* exposed to biocide stress reveals a multi-system response involving cell wall synthesis, sugar uptake, and motility. Front. Microbiol. 5 (FEB), 1–10. https://doi.org/10.3389/fmicb.2014.00068.
Chatterjee, S.S., Hossain, H., Otten, S., Kuenne, C., Kuchmina, K., Machata, S., Domann, E., Chakraborty, T., Hain, T., 2006. Intracellular gene expression profile of *Listeria monocytogenes*. Infect. Immun. 74 (2), 1323–1338. https://doi.org/10.1128/IAI.74.2.1323-1338.2006.
Chen, L., Zheng, D., Liu, B., Yang, J., Jin, Q., 2016. Vfdb 2016: hierarchical and refined dataset for big data analysis - 10 years on. Nucleic Acids Res. 44 (D1), D694–D697. https://doi.org/10.1093/nar/gkv1239.
Chiara, M., Caruso, M., D'Erchia, A.M., Manzari, C., Fraccalvieri, R., Goffredo, E., Latorre, L., Miccolupo, A., Padalino, I., Santagada, G., Chiocco, D., Pesole, G., Horner, D.S., Parisi, A., 2015. Comparative genomics of *Listeria* Sensu Lato: genus-wide differences in evolutionary dynamics and the progressive gain of complex, potentially pathogenicity-related traits through lateral gene transfer. Genome Biology and Evolution 7 (8), 2154–2172. https://doi.org/10.1093/gbe/evv131.
Cortes, B.W., Naditz, A.L., Anast, J.M., Schmitz-Esser, S., 2020. Transcriptome sequencing of *Listeria monocytogenes* reveals major gene expression changes in response to lactic acid stress exposure but a less pronounced response to oxidative stress. Front. Microbiol. 10 (January), 1–14. https://doi.org/10.3389/fmicb.2019.03110.
Cui, H., Li, H., Abdel-Samie, M.A., Surendhiran, D., Lin, L., 2021. Anti-*Listeria monocytogenes* biofilm mechanism of cold nitrogen plasma. Innovat. Food Sci. Emerg. Technol. 67 (July 2020), 102571 https://doi.org/10.1016/j.ifset.2020.102571.
Danecek, P., Bonfield, J.K., Liddle, J., Marshall, J., Ohan, V., Pollard, M.O., Whitwham, A., Keane, T., McCarthy, S.A., Davies, R.M., Li, H., 2021. Twelve years of SAMtools and BCFtools. GigaScience 10 (2), 1–4. https://doi.org/10.1093/gigascience/giab008.
Dar, D., Dar, N., Cai, L., Newman, D.K., 2021. Spatial transcriptomics of planktonic and sessile bacterial populations at single-cell resolution. Science 373 (6556). https://doi.org/10.1126/science.abi4882.
EFSA, ECDC, 2021. The European union one health 2020 zoonoses report. EFSA J. 19 (12) https://doi.org/10.2903/j.efsa.2021.6971.
Ercan, U.K., Sen, B., Brooks, A.D., Joshi, S.G., 2018. *Escherichia coli* cellular responses to exposure to atmospheric-pressure dielectric barrier discharge plasma-treated N-acetylcysteine solution. J. Appl. Microbiol. 125 (2), 383–397. https://doi.org/10.1111/jam.13777.
Evans, C.R., Kempes, C.P., Price-Whelan, A., Dietrich, L.E.P., 2020. Metabolic heterogeneity and cross-feeding in bacterial multicellular systems. Trends Microbiol. 28 (9), 732–743. https://doi.org/10.1016/j.tim.2020.03.008.
Ferreira da Silva, M., Ferreira, V., Magalhães, R., Almeida, G., Alves, A., Teixeira, P., 2017. Detection of premature stop codons leading to truncated internalin A among food and clinical strains of *Listeria monocytogenes*. Food Microbiol. 63, 6–11. https://doi.org/10.1016/j.fm.2016.10.033.
Fuchs, T.M., Eisenreich, W., Kern, T., Dandekar, T., 2012. Toward a systemic understanding of *Listeria monocytogenes* metabolism during infection. Front. Microbiol. 3 (FEB), 1–12. https://doi.org/10.3389/fmicb.2012.00023.
Gandra, T.K.V., Volcan, D., Kroning, I.S., Marini, N., de Oliveira, A.C., Bastos, C.P., da Silva, W.P., 2019. Expression levels of the agr locus and *prfA* gene during biofilm formation by *Listeria monocytogenes* on stainless steel and polystyrene during 8 to 48 h of incubation 10 to 37 °C. Int. J. Food Microbiol. 300 (February), 1–7. https://doi.org/10.1016/j.ijfoodmicro.2019.03.021.
Garmyn, D., Augagneur, Y., Gal, L., Vivant, A.L., Piveteau, P., 2012. *Listeria monocytogenes* differential transcriptome analysis reveals temperature-dependent Agr regulation and suggests overlaps with other regulons. PLoS One 7 (9). https://doi.org/10.1371/journal.pone.0043154.
Gay, C., Gebicki, J.M., 2000. A critical evaluation of the effect of sorbitol on the ferric–xylenol orange hydroperoxide assay. Anal. Biochem. 284 (2), 217–220. https://doi.org/10.1006/abio.2000.4696.
Griess, J.P., 1879. Bemerkungen zu der Abhandlung der HH: wesely und Benedikt "Ü ber einige Azoverbindungen. Ber. Deutsch. Chem. Ges. 12, 426–428.
Günther, F., Scherrer, M., Kaiser, S.J., DeRosa, A., Mutters, N.T., 2016. Comparative testing of disinfectant efficacy on planktonic bacteria and bacterial biofilms using a new assay based on kinetic analysis of metabolic activity. J. Appl. Microbiol. 625–633. https://doi.org/10.1111/jam.13358.
Handorf, O., Weihe, T., Freund, E., Riedel, K., Pauker, V.I., Weihe, T., Schäfer, J., Freund, E., Schnabel, U., Bekeschus, S., Riedel, K., Ehlbeck, J., 2021. Plasma-treated water affects *Listeria monocytogenes* vitality and biofilm formation. Front. Microbiol. 12 (April), 1–16. https://doi.org/10.3389/fmicb.2021.652481.
Herianto, S., Hou, C.Y., Lin, C.M., Chen, H.L., 2021. Nonthermal plasma-activated water: a comprehensive review of this new tool for enhanced food safety and quality. Compr. Rev. Food Sci. Food Saf. 20 (1), 583–626. https://doi.org/10.1111/1541-4337.12667.
Horlbog, J.A., Stevens, M.J.A., Stephan, R., Guldimann, C., 2019. Global transcriptional response of three highly acid-tolerant field strains of *Listeria monocytogenes* to HCl stress. Microorganisms 7 (10). https://doi.org/10.3390/microorganisms7100455.
Hozák, P., Scholtz, V., Khun, J., Mertová, D., Vaňková, E., Julák, J., 2018. Further contribution to the chemistry of plasma-activated water : influence on bacteria in planktonic and biofilm forms. Plasma Diagnostics 44 (9), 799–804. https://doi.org/10.1134/S1063780X18090040.
Hua, Z., Korany, A.M., El-Shinawy, S.H., Zhu, M.J., 2019. Comparative evaluation of different sanitizers against *Listeria monocytogenes* biofilms on major food-contact surfaces. Front. Microbiol. 10 (November), 1–8. https://doi.org/10.3389/fmicb.2019.02462.
Huang, Y., Morvay, A.A., Shi, X., Suo, Y., Shi, C., Knøchel, S., 2018. Comparison of oxidative stress response and biofilm formation of *Listeria monocytogenes* serotypes 4b and 1/2a. Food Control 85, 416–422. https://doi.org/10.1016/j.foodcont.2017.10.007.
Hyatt, D., Chen, G.-L., LoCascio, P.F., Land, M.L., Larimer, F.W., Hauser, L.J., 2006. Integrated nr database in protein annotation system and its localization. Comput. Eng. 6 (1), 1–8. https://doi.org/10.3969/j.issn.1000-3428.2006.05.026.
Karatzas, K.A.G., Suur, L., O'Byrne, C.P., 2012. Characterization of the intracellular glutamate decarboxylase system: analysis of its function, transcription, and role in the acid resistance of various strains of *Listeria monocytogenes*. Appl. Environ. Microbiol. 78 (10), 3571–3579. https://doi.org/10.1128/AEM.00227-12.
Koomen, J., den Besten, H.M.W., Metselaar, K.I., Tempelaars, M.H., Wijnands, L.M., Zwietering, M.H., Abee, T., 2018. Gene profiling-based phenotyping for identification of cellular parameters that contribute to fitness, stress-tolerance and virulence of *Listeria monocytogenes* variants. Int. J. Food Microbiol. 283 (May), 14–21. https://doi.org/10.1016/j.ijfoodmicro.2018.06.003.
Kragh, M.L., Truelstrup Hansen, L., 2020. Initial transcriptomic response and adaption of *Listeria monocytogenes* to desiccation on food grade stainless steel. Front. Microbiol. 10 (January), 1–20. https://doi.org/10.3389/fmicb.2019.03132.
Lamas, A., Regal, P., Vázquez, B., Miranda, J.M., Franco, C.M., Cepeda, A., 2019. Transcriptomics: a powerful tool to evaluate the behavior of foodborne pathogens in the food production chain. Food Res. Int. 125 (April), 108543 https://doi.org/10.1016/j.foodres.2019.108543.
Langmead, B., Salzberg, S.L., 2012. Fast gapped-read alignment with Bowtie 2. Nat. Methods 9, 357–359. https://www.nature.com/articles/nmeth.1923.
Lemon, K.P., Higgins, D.E., Kolter, R., 2007. Flagellar motility is critical for *Listeria monocytogenes* biofilm formation. J. Bacteriol. 189 (12), 4418–4424. https://doi.org/10.1128/JB.01967-06.
Li, Q., Liu, L., Guo, A., Zhang, X., Liu, W., Ruan, Y., 2021. Formation of multispecies biofilms and their resistance to disinfectants in food processing environments: a review. J. Food Protect. 84 (12), 2071–2083. https://doi.org/10.4315/jfp-21-071.
Li, Y., Pan, J., Wu, D., Tian, Y., Zhang, J., Fang, J., Paper, O., 2019. Regulation of *Enterococcus faecalis* biofilm formation and Quorum Sensing related virulence factors with ultra-low dose reactive species produced by plasma activated water. Plasma Chem. Plasma Process. 39 (1), 35–49. https://doi.org/10.1007/s11090-018-9930-2.
Liu, Y., Orsi, R.H., Gaballa, A., Wiedmann, M., Boor, K.J., Guariglia-Oropeza, V., 2019. Systematic review of the *Listeria monocytogenes* σ regulon supports a role in stress response, virulence and metabolism. Future Microbiol. 14 (9), 801–828. https://doi.org/10.2217/fmb-2019-0072.
López, M., Calvo, T., Prieto, M., Múgica-Vidal, R., Muro-Fraguas, I., Alba-Elías, F., Alvarez-Ordóñez, A., 2019. A review on non-thermal atmospheric plasma for food preservation: mode of action, determinants of effectiveness, and applications. Front. Microbiol. 10 (APR) https://doi.org/10.3389/fmicb.2019.00622.
Love, M.I., Huber, W., Anders, S., 2014. Moderated estimation of fold change and dispersion for RNA-seq data with DESeq2. Genome Biol. 15 (12), 1–21. https://doi.org/10.1186/s13059-014-0550-8.
Machado-Moreira, B., Tiwari, B.K., Richards, K.G., Abram, F., Burgess, C.M., 2021. Application of plasma activated water for decontamination of alfalfa and mung bean seeds. Food Microbiol. 96 (November 2020), 103708 https://doi.org/10.1016/j.fm.2020.103708.
Mai-Prochnow, A., Zhou, R., Zhang, T., Ostrikov, K., Ken), Mugunthan, S., Rice, S.A., Cullen, P.J., 2021. Interactions of plasma-activated water with biofilms:

inactivation, dispersal effects and mechanisms of action. Npj Biofilms and Microbiomes 7 (1), 1–12. https://doi.org/10.1038/s41522-020-00180-6.
Mazaheri, T., Cervantes-Huamán, B.R.H., Bermúdez-Capdevila, M., Ripolles-Avila, C., Rodríguez-Jerez, J.J., 2021. *Listeria monocytogenes* biofilms in the food industry: is the current hygiene program sufficient to combat the persistence of the pathogen? Microorganisms 9 (1), 1–19. https://doi.org/10.3390/microorganisms9010181.
Mellin, J.R., Koutero, M., Dar, D., Nahori, M.A., Sorek, R., Cossart, P., 2014. Sequestration of a two-component response regulator by a riboswitch-regulated noncoding RNA. Science 345 (6199), 940–943. https://doi.org/10.1126/science.1255083.
Moreno-Letelier, A., Olmedo, G., Eguiarte, L.E., Martinez-Castilla, L., Souza, V., 2011. Parallel evolution and horizontal gene transfer of the pst operon in Firmicutes from oligotrophic environments. Int. J. Evol. Biol. 2011, 1–10. https://doi.org/10.4061/2011/781642.
Naítali, M., Kamgang-Youbi, G., Herry, J.M., Bellon-Fontaine, M.N., Brisset, J.L., 2010. Combined effects of long-living chemical species during microbialinactivation using atmospheric plasma-treated water. Appl. Environ. Microbiol. 76 (22), 7662–7664. https://doi.org/10.1128/AEM.01615-10.
Oliveira, M., Fernández-Gómez, P., Álvarez-Ordóñez, A., Prieto, M., López, M., 2022. Plasma-activated water: a cutting-edge technology driving innovation in the food industry. Food Res. Int. 156 (February) https://doi.org/10.1016/j.foodres.2022.111368.
Pal, C., Bengtsson-Palme, J., Rensing, C., Kristiansson, E., Larsson, D.G.J., 2014. BacMet: Antibacterial biocide and metal resistance genes database. Nucleic Acids Res. 42 (D1), 737–743. https://doi.org/10.1093/nar/gkt1252.
Patange, A., O'Byrne, C., Boehm, D., Cullen, P.J., Keener, K., Bourke, P., 2019. The effect of atmospheric cold plasma on bacterial stress responses and virulence using *Listeria monocytogenes* knockout mutants. Front. Microbiol. 10 (December), 1–12. https://doi.org/10.3389/fmicb.2019.02841.
Sanchez-Vizuete, P., Orgaz, B., Aymerich, S., Le Coq, D., Briandet, R., 2015. Pathogens protection against the action of disinfectants in multispecies biofilms. Front. Microbiol. 6, 705. https://doi.org/10.3389/fmicb.2015.00705.
Seixas, A.F., Quendera, A.P., Sousa, J.P., Silva, A.F.Q., Arraiano, C.M., Andrade, J.M., 2022. Bacterial response to oxidative stress and RNA oxidation. Front. Genet. 12 (January), 1–12. https://doi.org/10.3389/fgene.2021.821535.
Sharmin, N., Pang, C., Sone, I., Walsh, J.L., Fernández, C.G., Sivertsvik, M., Fernández, E. N., 2021a. Synthesis of sodium alginate–silver nanocomposites using plasma activated water and cold atmospheric plasma treatment. Nanomaterials 11 (9). https://doi.org/10.3390/nano11092306.
Sharmin, N., Sone, I., Walsh, J.L., Sivertsvik, M., Fernández, E.N., 2021b. Effect of citric acid and plasma activated water on the functional properties of sodium alginate for potential food packaging applications. Food Packag. Shelf Life 29 (July). https://doi.org/10.1016/j.fpsl.2021.100733.
Shelton, A.N., Seth, E.C., Mok, K.C., Han, A.W., Jackson, S.N., Haft, D.R., Taga, M.E., 2019. Uneven distribution of cobamide biosynthesis and dependence in bacteria predicted by comparative genomics. ISME J. 13 (3), 789–804. https://doi.org/10.1038/s41396-018-0304-9.
Smet, C., Govaert, M., Kyrylenko, A., Easdani, M., Walsh, J.L., Van Impe, J.F., 2019. Inactivation of single strains of *Listeria monocytogenes* and *Salmonella* Typhimurium planktonic cells biofilms with plasma activated liquids. Front. Microbiol. 10 (July), 1–15. https://doi.org/10.3389/fmicb.2019.01539.
Steinegger, M., Söding, J., 2017. MMseqs2 enables sensitive protein sequence searching for the analysis of massive data sets. Nat. Biotechnol. 35, 1026–1028.
Stoll, R., Goebel, W., 2010. The major PEP-phosphotransferase systems (PTSs) for glucose, mannose and cellobiose of *Listeria monocytogenes*, and their significance for extra- and intracellular growth. Microbiology 156 (4), 1069–1083. https://doi.org/10.1099/mic.0.034934-0.
Tasaki, S., Nakayama, M., Shoji, W., 2017. Self-organization of bacterial communities against environmental pH variation: controlled chemotactic motility arranges cell population structures in biofilms. PLoS One 12 (3), 1–13. https://doi.org/10.1371/journal.pone.0173195.
Vaka, M.R., Sone, I., Álvarez, R.G., Walsh, J.L., Prabhu, L., Sivertsvik, M., Fernández, E. N., 2019. Towards the next-generation disinfectant: composition, storability and preservation potential of plasma activated water on baby spinach leaves. Foods 8 (12). https://doi.org/10.3390/foods8120692.
van der Veen, S., van Schalkwijk, S., Molenaar, D., de Vos, W.M., Abee, T., Wells-Bennik, M.H.J., 2010. The SOS response of *Listeria monocytogenes* is involved in stress resistance and mutagenesis. Microbiology 156 (2), 374–384. https://doi.org/10.1099/mic.0.035196-0.
Yost, A.D., Joshi, S.G., 2015. Atmospheric nonthermal plasma-treated PBS inactivates *Escherichia coli* by oxidative DNA damage. PLoS One 10 (10), 1–20. https://doi.org/10.1371/journal.pone.0139903.
Zetzmann, M., Bucur, F.I., Crauwels, P., Borda, D., Nicolau, A.I., Grigore-Gurgu, L., Seibold, G.M., Riedel, C.U., 2019. Characterization of the biofilm phenotype of a *Listeria monocytogenes* mutant deficient in agr peptide sensing. Microbiol. 8 (9), 1–9. https://doi.org/10.1002/mbo3.826.
Zhao, Y.-M., Patange, A., Sun, D.W., Tiwari, B., 2020a. Plasma-activated water: physicochemical properties, microbial inactivation mechanisms, factors influencing antimicrobial effectiveness, and applications in the food industry. Compr. Rev. Food Sci. Food Saf. 19 (6), 3951–3979. https://doi.org/10.1111/1541-4337.12644.
Zhao, Y.M., Ojha, S., Burgess, C.M., Sun, D.W., Tiwari, B.K., 2020b. Inactivation efficacy and mechanisms of plasma activated water on bacteria in planktonic state. J. Appl. Microbiol. 129 (5), 1248–1260. https://doi.org/10.1111/jam.14677.
Zhao, Yi Ming, Ojha, S., Burgess, C.M., Sun, D.W., Tiwari, B.K., 2021. Inactivation efficacy of plasma-activated water: influence of plasma treatment time, exposure time and bacterial species. Int. J. Food Sci. Technol. 56 (2), 721–732. https://doi.org/10.1111/ijfs.14708.
Zhou, R., Zhou, R., Prasad, K., Fang, Z., Speight, R., Bazaka, K., Ostrikov, K., 2018. Cold atmospheric plasma activated water as a prospective disinfectant: the crucial role of peroxynitrite. Green Chem. 20 (23), 5276–5284. https://doi.org/10.1039/c8gc02800a.